JPET Fast Forward. Published on November 20, 2008 as DOI: 10.1124/jpet.108.146365

Pharmacological characterization of pannexin-1 currents expressed in mammalian cells

Weihong Ma, Hui Hui, Pablo Pelegrin and Annmarie Surprenant

Faculty of Life Sciences, Michael Smith Building, University of Manchester, Manchester M13 9PT, United Kingdom (W.M., H.H., P.P., A.S.)

Running title: inhibition of panx1 currents

Corresponding author: Annmarie Surprenant, Faculty of Life Sciences, Michael Smith Building D3315, University of Manchester, Manchester, M13 9PT, United Kingdom. Phone: 44-161-306-0505 Fax: 44-161-275-1498.

Email: a.surprenant@manchester.ac.uk

Number text pages: 31

Number tables: 1

Number figures: 7

Number references: 21

Number words in Abstract: 232

Number words Introduction: 713

Number words Discussion: 1576

Abbreviations: panx1, pannexin1; CBX, carbenoxolone; MFQ, mefloquine; PPi, pyrophosphate; U73122, 1-[6-((17β-3-methoxyestra-1,3,5(10)-trien-17-yl)amino)hexyl]-1H-pyrrole-2,5-dione; U73343, 1-[6-((17β-3-Methoxyestra-1,3,5(10)-trien-17-yl)amino)hexyl]-2,5-pyrrolidinedione; NPPB, 5-Nitro-2-(3-phenylpropylamino)benzoic acid; DIDS, disodium 4,4'-diisothiocyanatostilbene-2,2'-disulfonate; SITS, disodium 4-acetamido-4'-isothiocyanato-stilben-2,2'-disulfonate; IAA-94, Indanyloxyacetic acid 94; FFA, flufenamic acid; NFA, niflumic acid; 9-AC, anthracene-9-carboxylic acid; DPC, diphenylamine-2-carboxylate.

Section assignment: Cellular and molecular

Abstract

Pannexin 1 (Panx1) is a widely expressed protein that shares structural, but not amino acid, homology with gap junction proteins, the connexins. Panx1 does not form gap junctions in mammalian cells but it may function as a plasma membrane hemichannel. Little is known of the pharmacological properties of panx1 expression in mammalian cells. Here we identify three variants in the human *PANX1* gene. We expressed these variants and mouse Panx1 in mammalian cells and compared Panx1-induced currents. All human Panx1 variants and the mouse Panx1 showed identical protein expression levels, localization patterns, and functional properties although the frequency of functional expression was species-dependent. Panx1 currents were independent of changes in extracellular or intracellular calcium or phospholipase C transduction. We found compounds that inhibited Panx1 currents with a rank order of potency: CBX > DIDS ≈ SITS ≈ NPPB > IAA-94 >> probenecid >> FFA = NFA. Triphosphate nucleotides (ATP, GTP and UTP) rapidly and reversibly inhibited Panx1 currents via mechanism(s) independent of purine receptors. When Panx1 was co-expressed with $P2X_7R$, DIDS was found to act as a $P2X_7R$ antagonist to inhibit ATP-evoked currents, but none of the other compounds inhibited $P2X_7R$ currents. This is the first detailed pharmacological characterization of Panx1 mediated currents in mammalian cells and sheds new, though contradictory, light on the hypothesis that Panx1 acts as a hemichannel to allow passage of large molecules in response to $P2X_7R$ activation.

Introduction

Pannexins are a three-membered family of membrane proteins (Panx1, 2, 3) that bear topological similarity, but minimal amino acid homology, to the large family of gap-junction channels, the connexins (Panchin, 2005; Barbe et al., 2006). Unlike connexins, pannexins do not form gap junctions when expressed in mammalian cells (Huang et al., 2007b) but do lead to the appearance of ionic currents whose properties resemble "undocked" gap-junction hemichannels (Scemes et al., 2007). Panx1 has distinct but generally ubiquitous expression in excitable and non-excitable cells and has generated increasing interest as a likely hemichannel conduit for non-vesicular release of ATP from erythrocytes and taste receptor cells (Locovei et al., 2006a; Huang et al., 2007b). Panx1 has also been shown to form protein-protein association with the purinergic $P2X_7$ receptor ($P2X_7R$) whose activation by extracellular ATP opens a typical cationic channel within ms followed seconds later by an opening, or activation, of a large pore permeable to molecules up to 900 dalton (Pelegrin and Surprenant, 2006). The initial phase of this $P2X_7R$-activated dye-permeable pore is inhibited by blockade of Panx1 using siRNA knockdown techniques, by a Panx1-mimetic inhibitory peptide, and by the relatively non-selective gap-junction channel blocker, CBX (Pelegrin and Surprenant, 2006, 2007). These results have provided the evidence for the hypothesis that Panx1 hemichannels open in response to conformational changes of the $P2X_7R$ protein complex upon its activation, thus allowing passage of the larger molecules through its open hemichannel (Pelegrin and Surprenant, 2006; Scemes et al., 2007). Mechanical and osmotic stimuli as well as changes in intracellular calcium have also been suggested to open Panx1

hemichannels in the absence of $P2X_7R$ presence or activation (Locovei et al., 2006b; Vanden Abeele et al., 2006).

Because the molecular identification of pannexins has occurred relatively recently (Bruzzone et al., 2003; Baranova et al., 2004), there have been few pharmacological characterizations of ectopically expressed Panx1 currents, and all have been carried out using the oocyte expression system (Bruzzone et al., 2005; Locovei et al., 2006b; Silverman et al., 2008), with the exception of our previous study of human Panx1 currents expressed in HEK293 cells (Pelegrin and Surprenant, 2006). Expression of Panx1 in either oocytes or mammalian cells results in ionic currents that are in general agreement; that is, currents activate upon depolarizations greater than ~ 10 mV, show minimal time dependence of activation, are rapidly and reversibly inhibited by carbenoxolone (CBX) at concentrations (EC_{50} ~ 5 μM) that are 5 – 20-fold less than required to inhibit connexin-mediated currents, are independent of external calcium, and are only weakly inhibited by flufenamic acid, a commonly used inhibitor of both chloride channels and gap-junction channels (Bruzzone et al., 2005). Few other pharmacological properties of Panx1-mediated currents are known, although probenecid, a compound long used clinically for the treatment of gout, and thought to act by inhibiting specific plasma membrane anionic transporters, has recently been shown to block Panx1 currents in oocytes without inhibiting connexin (46 and 32) currents (Silverman et al., 2008). In contrast, there appear to be striking discrepancies in results obtained from oocyte expression and mammalian cell expression when $P2X_7R$ is co-expressed with Panx1. In the oocyte expression system, currents in response to ATP activation of ectopically expressed $P2X_7R$ is inhibited by CBX and mefloquine (Iglesias et al., 2008), but in

mammalian expression systems no inhibition of $P2X_7R$-mediated currents by these compounds is observed (Pelegrin and Surprenant, 2006).

The present study was undertaken in order to expand the currently limited repertoire of compounds that may act on Panx1, particularly in mammalian cell expression systems. We carried out quantitative comparisons of currents induced by expression of human and mouse Panx1 in HEK293 cells (in the absence of $P2X_7R$). We found that ATP and other nucleotides directly inhibited both human and mouse Panx1 currents in a purine receptor-independent manner, that Panx1 currents were independent of intracellular calcium concentrations, and that some non-selective chloride channel inhibitors (NPPB, DIDS, IAA-94), blocked Panx1 currents while others (FFA, NFA, 9-AC, MFQ and DPC) had little or no effect. DIDS, but none of the other compounds, inhibited $P2X_7R$-mediated currents in cells expressing only $P2X_7R$ or in cells co-expressing both $P2X_7R$ and Panx1. These results expand the previously limited pharmacological profile of panx1 currents, and show that inhibition of panx1 currents are independent of inhibition of $P2X_7$ receptor currents.

Methods

Materials. All salts and compounds used in this study were from Sigma-Aldrich (UK) except for DPC from Merck (UK), U73122 and U73343 from Calbiochem (UK). Panx1 antibodies were from Santa Cruz Biotechnology (USA), Millipore (UK), Diatheva (Italy), or generously supplied by S. Scherer (University of Pennsylvania). Secondary Abs were from DakoCytomation (UK), all cell culture media, Optimem and Lipofectamine 2000 were from Invitrogen (UK).

Cells, transfections, cloning and siRNA. HEK293 cells were originally obtained from ATCC (UK) and maintained as previously described (Pelegrin and Surprenant, 2006). Transient transfection was carried out similarly for all cell lines using Lipofectamine 2000 (Gibco-Invitrogen), as described in detail previously (Roger et al., 2008). Unless otherwise stated, Panx1 cDNA (1 μg) was co-transfected with eGFP (0.1 μg), and electrophysiological recordings were made 24 – 48 hours post-transfection. siRNA for human Panx-1 has been described (Pelegrin and Surprenant, 2006). Human Panx-1 expression vectors have been described (Pelegrin and Surprenant, 2006); the full-length sequence encoding mouse Panx-1 was amplified from total mouse C57 BL/6 brain mRNA using RT-PCR and cloned into pcDNA3.1(-) vector (Invitrogen). c-myc (EQKLISEEDL) and eGFP tags were introduced in frame at the 3'-end of the coding sequence of mouse Panx-1 using overlapping PCR and Accuzyme^{TM} proof-reading DNA polymerase (Bioline); DsRed tag was introduced in frame at the 3'-end of the coding sequence of human Panx-1; FLAG tag (DYKDDDDK) was introduced in the second extracellular loop of human Panx-1-myc at position 162-168; hence, incorporating a c-myc, eGFP or DsRed fusion tag at the C terminus or a FLAG tag at the second

extracellular loop of the expressed protein. The different human Panx-1 splice variants and the deletion of V377 were generated from the hPanx-1-ee construct using the PCR overlap extension method (Young et al., 2007) and Accuzyme^{TM} DNA polymerase. Cloned products were confirmed by sequencing (Beckman-Coulter CEQ 2000 Dye Terminator) and protein expression was verified by Western blotting.

Immunohistochemistry. For immunohistochemistry, cells were transfected as described above on coverslips or in 35mm Petri dishes and plated onto coverslips 4h post transfection; cells were examined 24-48 h later. Cells were washed twice with PBS followed by fixation (4% v/v formaldehyde in PBS) for 30 min at room temperature, then permeabilised with blocking solution (0.1% Triton X-100 and 0.3% BSA in PBS) for 40 min. Cells were then incubated with primary Ab against Myc-tag (1:1000 in the blocking solution) for 1h at room temperature. After washing three times with PBS, anti-mouse IgG Alexa Fluor 594 conjugated secondary Ab (1:200; Invitrogen) was applied for 30 min. DAPI (Invitrogen) was used for nuclear staining. After brief rinse in H_2O, coverslips were mounted on slides with Gold antifade reagent (Invitrogen). Cells were photographed using Zeiss Plan-Neofluar 100x oil and AxioVision software (Zeiss UK), Nikon Eclipse TE300 confocal 60X objective and EZ-C1 software (Nikon UK) or Olympus IX71 100x objective with SoftWoRx 3.5 (Deltavision, UK), as indicated. We generated several epitope-tagged Panx1 proteins; there were no differences between human and mouse Panx1 protein localization when expressed in HEK293 cells (Supplemental Fig. 1). C-terminal fusion of large epitopes (eGFP or DsRed) resulted in panx1 protein remaining intracellular in vacuole-like compartments while smaller

epitopes (c-myc or ee-tags) showed intense, plasma membrane-delimited expression (Supplemental Fig 1A,B).

Reverse transcription and PCR analysis. Human brain RNA (Ambion) and total RNA from other cells were isolated using RNeasy Mini kit (Qiagen), followed by reverse transcription using SUPERSCRIPT^{TM} III (Invitrogen) RNase H-reverse transcriptase with oligo-dT. Genomic DNA was isolated by digesting 10^6 cells in a buffer containing 23 mg/ml of proteinase K and 0.5% triton X-100 at 56^{o}C for 60 min. Panx-1 was amplified by standard PCR protocols from cDNA using specific oligonucleotides that differentiate between the alternative splice variant on exon 5 (F1/Ra or F1/Rb, Supplemental Table 1) or the deletion of a single Val at position 377 in exon 4 (F1/Rvv or F1/Rv, Supplemental Table 1); oligonucleotides annealing at both sides of intron 4 (F4/R2, Table 1) were used to amplify human Panx-1 from genomic PCR, this fragment contains V377 position in the exon 4; β-actin primers has been reported previously (Pelegrin and Surprenant, 2006). The PCR conditions to distinguish between the different Panx-1 variants were 20 cycles with a stringent annealing temperature of 65^{o}C for the a/b splicing variant and 70^{o}C for the V377 deletion. The obtained product sizes for all PCR products were as expected from their mRNA sequence or from the genomic DNA and were for F1/Ra 675 bp (panx1a); for F1/Rb 690 bp (panx1b) or 687 bp (panx1bv); for F1/Rvv 610 bp (panx1b); for F1/Rv 607 bp (panx1bv); for F4/Rvv 445 bp (panx1b); for F4/Rv 442 bp (panx1bv); for F4/R2 1110 bp (panx1b), 1098 bp (panx1a) and 1107 (panx1bv); and 1129 bp for β-actin.

Electrophysiology. Whole cell patch-clamp recordings were made at room temperature using an EPC9 amplifier, Pulse acquisition software (HEKA, Germany) and

AxographX analysis software (AxoGraph Scientific, Australia) as detailed recently (Roger et al., 2008). Membrane potential was held at -60 mV unless otherwise indicated. Compounds were applied by RSC fast flow system (Biologique, Grenoble France); drug equilibration time ranged from 20 ms – 1 s depending on distance of fast-flow tube from the recorded cell. We also superfused compounds for 3 – 6 min in addition to fast-flow application for those compounds that showed little or no effect in order to ensure complete drug access and equilibration. Recordings were made only from single cells in order to rule out possible contributions due to electrical coupling between cells, and in the majority of recordings the cell was lifted up from the coverslip after obtaining whole-cell configuration in order to further ensure complete drug delivery and confirm absence of coupled cells. Cells were chosen of approximately similar size and shape throughout this study; accordingly, whole-cell membrane capacitance showed minimal variability (range 8 – 12 pF, mean ± sem 9.6 ± 0.2 pF), therefore all results are shown as absolute current values. Standard intracellular/extracellular solutions were (mM): 147 NaCl, 10 HEPES, 10 EGTA/147 NaCl, 2 KCl, 1 $MgCl_2$, 2 $CaCl_2$, 10 HEPES and 13 glucose; intracellular calcium concentrations were calculated using WebMaxC software (http://www.stanford.edu/~cpatton/maxc.html). All solutions were at pH 7.3 and 300-315 $mosmol^{-1}$. In most experiments voltage ramps (-120 – 80 mV) were applied at 2 – 10 s intervals after steady-state dialysis of internal solutions had been attained, usually within 2 – 3 min after obtaining whole-cell conditions. Voltage steps (20 mV increments at 1 s intervals from -120 to 80 mV) were also applied before, during and after application of compounds. Concentration-response inhibition curves were determined by least squares fit to the Hill equation: $I/I_{max} = 1/[1+(B/IC_{50})^n]$, where I is the current as a

fraction of control (I_{max} at 70 mV) and *B* is the concentration of inhibitor. Figures show curves fitted to the mean of all experiments; Kaleidagraph software (Synergy Software USA) was used for curve fitting and statistical analysis via Student's *t*-test.

Fura2 calcium assay. Cells were plated in a 96-well black assay plate with clear bottom (Corning, USA) and cultured overnight to reach 90~100% confluency. Cells were pre-incubated with 4 μM Fura-2 AM (Molecular Probes, UK) at 37 ºC for 30 minutes. Prior to recording, Fura-2 AM was removed and replaced with the standard extracellular solution. Fluorescence was recorded by an automatic fluorescence plate reader, FlexStation 3 (Molecular Devices, USA) over 5 to 10 minutes at 4 s intervals. The dual excitation for Fura-2 was 340 nm/380 nm and the emission 510 nm. Agonists were added into the wells automatically by the machine at designated time points whereas any antagonists were added to the wells 5 minutes before recording started. Data were acquired by the SoftMax Pro 5 software and the intracellular calcium level was expressed as the ratio of the emission intensities for 340 and 380 nm.

Results

Splice variants and single nucleotide polymorphism in human Panx1. It has been reported that human Panx1 presents an alternatively spliced exon 5 leading to the synthesis of Panx1 with two intracellular C-terminus lengths: Panx1a and Panx1b containing a 4 amino acid insert (GMNI) at position 400 (Fig.. 1A; Baranova et al., 2004). We examined the expression of these two variants in different human cell lines (HEK293, HeLa and THP-1) and in total human brain by using oligonucleotides to specifically amplify by PCR both splicing variants (Supplemental Table 1), and confirmed the selectivity of both oligonucleotide pairs by amplifying an expression vector carrying either human Panx1a or Panx1b coding sequence (Fig. 1B). Surprisingly, there was no expression of Panx1a in any cell line or tissue examined (Fig. 1B), although Panx1b was strongly expressed in all preparations (Fig. 1C). Both variants similarly trafficked to the plasma membrane when tagged with c-myc or ee-epitopes as revealed by immunocytochemistry in HEK293 cells expressing either Panx1a or b (Fig. 1D). We initially cloned human Panx1 from THP-1 macrophage cell line (Pelegrin and Surprenant, 2006) and noted that some clones contained a Panx1 coding sequence carrying a deletion of a single valine in the intracellular C-terminus domain at position 377 (Panx1bv; Fig. 1A). By using specific oligonucleotides (Supplemental Figure 2) we were able to differentially amplify both Panx1 variants from cDNA or genomic DNA. We found that HEK293 and THP-1 cells express both versions VV377/378 (Panx1b) and single V377 (Panx1bv) mRNAs, while HeLa cells or human brain express only Panx1b mRNA (Fig. 1B). Genomic differential amplification for V377 deletion revealed that THP-1 cells carry both versions in their genome and, as expected, HeLa cells only presented with the

Panx1b version (Fig. 1C). Localization of human Panx1bv was found in the plasma membrane, similar to Panx1b (Fig. 1D), indicating no major trafficking defects in Panx1 by the deletion of V377.

Functional expression of human and mouse Panx1. Transient transfection of mPanx1 (untagged, ee, or c-myc tagged) in HEK293 cells resulted in appearance of a distinct current whose properties were virtually identical to those previously described for heterologous expression of hPanx1 in HEK293 cells (Pelegrin and Surprenant, 2006). The Panx1-associated current activated at membrane potentials > 10 mV, showed no desensitization during maintained depolarizations for up to 1 min, and was rapidly (within 10 ms) and reversibly (within 1 s) blocked by CBX (30 or 50 μM) (Fig. 2A). In approximately 50% of Panx1 or vector-transfected cells and 20% of untransfected cells, a lanthanum-sensitive inward current was apparent (Fig. 2A). In the absence of lanthanum this current was increased by up to 10-fold by CBX (data not shown); therefore, we used lanthanum (2 mM) in all solutions when this Panx1-independent current was observed. Lanthanum had no effect on the CBX-inhibited outward current recorded in Panx1-transfected cells (Fig. 2A), nor did it alter the actions of any of the compounds we examined in the present study. We therefore defined the difference between the current in the presence of 2 mM lanthanum and the current in the presence of 2 mM lanthanum plus 50 μM CBX as the Panx1 current. Although both human and mouse Panx1 protein showed intense plasma membrane localization in > 95% of all transfected cells, (e.g. Supplemental Fig. 1), the frequency of recording hPanx1-associated currents was very low (8-35% of cells) compared with mPanx1-transfected cells (80-85% of cells, Fig. 2D). No hPanx1-mediated currents were recorded from hPanx1-eGFP transfections and only

2/30 mPanx1-GFP cells exhibited currents (Fig. 2D), thus confirming the minimal to absent functional expression of these epitope-tagged proteins. However, when all other data were considered (i.e. excluding GFP and DsRed-tagged cDNA), there were no significant differences in average or maximum current amplitudes of Panx1-associated currents in cells transfected with any of the human or mouse Panx1 constructs (Fig. 2E).

Panx1 currents are calcium-independent. Changing extracellular calcium concentration from control (2 mM) to 10 mM or to calcium-free/1 mM EGTA solution did not alter hPanx1 or mPanx1 currents (n = 9 – 15 for each, Fig. 3A). We also did not observe any differences in average or maximum current amplitudes of Panx1 currents from cells dialysed with low intracellular calcium (calculated < 1 nM) or with high intracellular calcium (calculated 720 nM; Fig. 3A). However, it has been reported that activation of PLC-coupled metabotropic P2Y receptors leads to activation of human Panx1 when expressed in oocytes (Locovei et al., 2006b). Therefore, we examined in more detail possible modulation of Panx1 currents by altered intracellular calcium concentrations by using the PLC inhibitor U73122. Application of U73122 to untransfected, vector-transfected or Panx1-transfected HEK293 cells resulted in a time-dependent increase in inward and outward currents; lanthanum (2 mM) completely blocked these U73122-induced currents (Fig. 3B), and were therefore not attributed to panx1 activation. After blockade of the Trp-like currents with lanthanum (Fig. 3C), U73122 now produced a time-dependent inhibition of the Panx1-associated current; the maximum inhibition by U73122 (10 μM) was 80% of the inhibition produced by CBX (Fig. 3D). The time constant of inhibition was 1.3 min (Fig. 4). Neither the kinetics of U73122 inhibition nor the maximum inhibition was altered by dialysing cells with low (<

1 nM) or high (720 nM) intracellular calcium. Similarly, no changes occurred when external calcium was removed in addition to treating cells with BAPTA-AM (Fig. 4A). Moreover, U73343 (10 μM), an inactive analogue of U73122 in terms of PLC inhibition, was equally effective to inhibit Panx1 currents although with slower kinetics (time constant of inhibition 2.5 min; Fig. 4B). We confirmed the selective effectiveness of U73122 in blocking P2Y-mediated calcium transients from untransfected, vector-transfected and Panx1-transfected HEK cells and found that a 5 min exposure to a 10 μM concentration of U73122 blocked 95-100% of the ATP-evoked calcium responses, while the same concentration of the PLC-inactive analogue, U73343, had no effect (Supplemental Fig. 3).

Inhibition of Panx1 currents by non-selective chloride channel/anion transporter blockers. We examined a number of compounds that are known to inhibit gap junctions, cation and anion transporters, Trp channels and chloride channels, all of which are relatively non-selective but which may provide a "Panx1-specific repertoire". Examples of two compounds, NPPB and SITS, which were effective inhibitors of mouse and human Panx1 currents are shown in Fig. 5A, concentration-inhibition curves for compounds that inhibited Panx1 currents are shown in Fig. 5B, and inhibitor potencies are shown in Fig. 5C and Table 1. The most potent inhibitor was CBX (IC_{50} 5 μM) and the weakest probenecid (IC_{50} 350 μM). Lanthanum (2 mM, Fig. 2, 3), gadolinium (300 μM), 2-APB, 9-AC and DPC (all at 100 μM) were without effect (data not shown, n = 4 – 6) .

Inhibition of Panx1 currents by nucleoside triphosphates. We examined the actions of ATP on Panx1 currents with the hypothesis that it was likely to directly

activate Panx1 currents. To our surprise, ATP, UTP and GTP, but not ADP, AMP, adenosine, pyrophosphates or monophosphates, rapidly and reversibly inhibited Panx1 currents with kinetics similar to CBX (Fig. 6). Maximum inhibition by ATP was 90% of CBX inhibition, while maximum inhibition by GTP or UTP was 70% of CBX inhibition (Fig. 6C,E). BzATP at 300 μM and 1 mM inhibited panx1 currents by 14 ± 4% and 36 ± 6% (*n* = 3) respectively; these concentrations of ATP-γ-S inhibited panx1 currents by 24 ± 5% and 46 ± 6% (*n* = 3) and αβ-meATP (0.5 mM) also inhibited panx1 currents by 34 ± 3% (*n* = 3). It was not economically feasible to examine higher concentrations of these analogues. There were no significant differences in ATP concentration-inhibition curve or kinetics of ATP inhibition when high concentrations of ATP were included in the recording pipette (10 – 20 mM, *n* = 17 for mPanx1 and 14 for hPanx1; Fig. 6D); intracellular ATP also did not alter the average or maximum Panx1 currents. The simultaneous inclusion of non-selective purine receptor antagonists, suramin (200 μM) and PPADS (100 μM) did not alter the inhibition by ATP, GTP or UTP (*n* = 2 for each nucleotide).

Actions of Panx1 inhibitors on $P2X_7R$-mediated currents. We examined the actions of compounds that inhibited Panx1-currents on ATP-evoked currents in cells co-expressing rat $P2X_7R$ + mPanx1, human $P2X_7R$ + mPanx1, mouse $P2X_7R$ + mPanx1 and rat $P2X_7R$ + hPanx1. In all these cells, a CBX- sensitive Panx1 current was recorded in the absence of ATP (data not shown). ATP evoked typical $P2X_7R$-mediated currents (Fig. 7A). CBX, NPPB, FFA, MFQ, NFA, and probenecid had no effect, or increased by 10 – 20% the peak current in response to ATP (Fig. 7A, table 1). In contrast, DIDS

JPET Fast Forward. Published on November 20, 2008 as DOI: 10.1124/jpet.108.146365
This article has not been copyedited and formatted. The final version may differ from this version.

readily inhibited $P2X_7R$-mediated currents (Fig. 7B,C) with IC_{50} values that were 10 to 20-fold higher than IC_{50} values for inhibition of Panx1 currents (Fig. 7C, table 1).

Discussion

This study provides the first detailed pharmacological characterization of Panx1-associated currents in mammalian cells, and presents results that may call for revision of current hypotheses regarding Panx1 function.

Protein and functional expression of Panx1 variants. Human Panx1 presents an alternatively spliced exon 5 which leads to a 4 amino acid insert (GMNI) within the intracellular C-terminus (Panx1b; Fig. 1A). This splicing variant was initially characterized by expressed sequences tags (ESTs) database searches (Baranova et al., 2004), however, no protein or functional expression studies of this Panx1b variant have been carried out previously. In the present study we examined several different human cell lines and brain tissue and found that Panx1b is the only Panx1 present. Although the initial report by Baranova et al. (2004) suggested the Panx1a splice variant is the more common form, our study reveals it is the Panx1b variant that should be considered to be most prominent. We also identified a novel difference in the intracellular C-terminus of human Panx1: a specific deletion of valine at position 377 (Panx1bv). The V377 coding sequence is present in exon 4 and the lack of this amino acid cannot be explained by an alternative spliced exon. However, the two consecutive valines at positions 377 and 378 present in the human Panx1 sequence (accession numbers AAK91713 and NP_056183) are encoded by a duplication of the same codon GTT at position 1131 in the coding sequence, therefore there are 4 different possibilities for a trinucleotide deletion to occur in that position to produce a single valine at position 377 (GTT^{1131}, GTT^{1134}, TTG^{1132} or TGT^{1133}). Both forms of Panx1, b and bv, were expressed in HEK293 and THP-1 human

cell lines. Coding sequences for both variants were found in THP-1 genomic DNA, indicating that these cells carry V377 deletion only in one allele of the *PANX1* gene. We were unable to detect expression of Panx1bv from HeLa cells or from brain and further studies will be needed to explore if Panx-1bv is present in the human population. In any case, all Panx1 variants (Panx1a, Panx1b and Panx1bv) were found to be equally trafficked to the plasma membrane (unless fused with GFP or DsRed) and they all showed the same electrophysiological profile, indicating that their functional properties remain the same irrespective of the Panx1 splice variant expressed in a specific tissue or the presence of Panx1bv in the genome.

Inhibition of Panx1 currents by chloride channel/transporter/gap junction channel blockers. We identified a number of compounds that reversibly inhibited Panx1 currents (Table 1); all are known to inhibit rather non-selectively gap junction channels, chloride channels and/or anion transporters. The rank order of potency for inhibition of either human or mouse Panx1 currents was CBX > DIDS ≈ SITS ≈ NPPB > IAA-94 >> probenecid >> FFA = NFA. However, not all gap junction/chloride channel blockers were effective, as heptanol, 9-AC, MFQ and DPC did not alter human or mouse Panx1 currents, nor did the non-selective Trp-channel/voltage-gated calcium channel blockers, lanthanum and gadolinium. Therefore, the profile presented by the above repertoire of inhibitors provides a useful pharmacological fingerprint to identify and distinguish native Panx1 currents. Although we have not examined directly mechanisms of inhibition by any of these compounds, the ms on and off-rates of inhibition by CBX, NPPB and DIDS suggest direct channel block. Probenecid, recently shown to block Panx1-induced but not connexin-mediated currents when expressed in oocytes (Silverman et al., 2008), showed

much slower kinetics with on and off rates in the minute domain, suggesting a distinct mechanism of inhibition. Because probenecid had previously been considered to act solely through anion transporter inhibition, Silverman et al. (2008) have raised the possibility that Panx1 may function as an essential component in a transport protein complex rather than as a separate permeation pathway. Our results add weight to this possibility because all the compounds (except CBX) we found to inhibit Panx1 currents are also known to inhibit various anion transporters, and other members of the ABC family of transporters (Kidd and Thorn, 2000; Strange et al., 1996; Gelband et al., 1996). It is not known whether CBX alters transporter functions because no studies examining actions of CBX on anion or other types of transporters have been carried out to date.

Calcium independence. Panx1 currents were unaltered by increasing or removing extracellular calcium, by markedly reducing levels of intracellular calcium (to < 1 nM) via dialysis with high concentrations of BAPTA or by loading cells with BAPTA-AM, or by greatly increasing intracellular calcium levels via dialysis of μM concentrations of calcium. Although studies to date on Panx1 function are in agreement that Panx1 currents are not modulated by extracellular calcium (Bruzzone et al., 2005; Pelegrin and Surprenant, 2006), it has been reported that Panx1 currents in oocytes can be activated by increased intracellular calcium, particularly by activation of the PLC pathway by purinergic P2Y receptors (Locovei et al., 2006b). In the present study, we further examined the actions of the PLC inhibitor, U73122, and found it did inhibit Panx1 currents but the inhibition was not via PLC transduction because the PLC-inactive analogue, U73343, was equally effective in blocking Panx1 currents and the U73122-induced inhibition of currents did not depend on levels of intracellular calcium. Thus, the

inhibition of Panx1 currents by U73122 and U73343 is independent of modulation of intracellular calcium, and likely reflects direct modulation of the Panx1 protein or protein complex itself.

Nucleotide inhibition of Panx1 currents and involvement of Panx1 in $P2X_7R$ function. In cells expressing Panx1 (but lacking $P2X_7R$), trinucleotides all rapidly and reversibly inhibited Panx1 currents in a manner similar to that observed for CBX. Although HEK293 cells are well known to endogenously express several P2Y receptors (but not P2X receptors), the nucleotide inhibition of Panx1 was clearly not mediated via activation of any metabotropic P2Y receptor because inhibitory concentrations of ATP, GTP and UTP were 50 - 100-fold greater than required to activate P2Y receptors, because GTP does not activate P2Y (or P2X) receptors, and because the combined application of suramin and PPADS did not alter the inhibitory actions of these trinucleotides. The rapid kinetics of the nucleotide inhibition, the high concentrations required, and the lack of effect of intracellular ATP are in keeping with direct channel block as the most likely mechanism of action. There are several examples of similar blockade of channel activity by ATP, particularly at chloride channels (e.g. Jackson and Strange, 1995).

ATP rapidly and reversibly inhibited Panx1 currents over the same concentration range (IC_{50} = 750 μM) that activates $P2X_7R$ receptor-channels. This result was unexpected because our previous results had led us to hypothesize that activation of $P2X_7R$ by extracellular ATP induced the opening of Panx1 channels which allowed passage of higher molecular weight molecules (up to 900 dalton). The evidence for this hypothesis was that Panx1 and $P2X_7R$ showed protein-protein interaction, and that CBX,

siRNA directed against Panx1, and a Panx1-mimetic peptide all inhibited the early dye-uptake associated with $P2X_7R$ activation without altering $P2X_7R$ currents or calcium flux (Pelegrin and Surprenant, 2006). In the present study, we again found that CBX produced a small *increase* in peak ATP-evoked currents in cells co-transfected with any combination of mouse, rat and human $P2X_7R$ with mouse or human Panx1 although the Panx1 currents recorded (in the absence of ATP) in the same cells showed the same CBX-induced inhibition as was observed in cells expressing only Panx1. Similar small increases in ATP-evoked currents occurred in the presence of NPPB, FFA and probenecid although DIDS inhibited $P2X_7R$-mediated currents in a concentration-dependent manner, thus demonstrating that DIDS is an effective $P2X_7R$ antagonist. Irrespective of the small increase in ATP-gated currents in $P2X_7R$-expressing cells by panx1 blockers, these results show clearly that, with the exception of DIDS, blockers of panx1 currents do not inhibit $P2X_7R$. Is it possible to reconcile these results with the hypothesis that activation of Panx1 hemichannels in response to $P2X_7R$ stimulation provide the conduit for dye-uptake? That is, ATP potently inhibits Panx1 currents in cells lacking $P2X_7R$ at the same concentrations that activate the $P2X_7R$ and its subsequent downstream signalling to dye-uptake. We believe these results are not compatible with Panx1 acting as a dye-permeable hemichannel although it is possible to imagine a situation where two functionally distinct populations of Panx1 hemichannels exist: one population associating within the $P2X_7R$ protein complex whose conformation does not allow direct ATP binding (so it opens in response to $P2X_7R$ activation) but retains inhibitory actions of CBX/NPPB/probenecid, and a second population that does not associate with $P2X_7R$ and is available for direct ATP inhibition by these panx1

blockers. However, we think it more likely that there remain one (or more) yet-to-be-identified molecule(s) that link Panx1 to $P2X_7R$-mediated dye-uptake and other downstream signalling cascades initiated by $P2X_7R$. We predict at least one of these postulated Panx1-$P2X_7R$ interacting proteins will be a type of anion transporter. Mutagenesis approaches designed to delineate residues in the Panx1 protein that are sites of interaction for ATP and other inhibitory compounds, and to determine regions that can be directly associated with ion flux should provide important information concerning how Panx1 may (or may not) function as an ion channel. Proteomic approaches aimed at identifying proteins associated within a $P2X_7R$-Panx1 co-complex should provide new candidates that may clarify how Panx1 is modulated by, or itself modulates, the $P2X_7R$. Most pertinently, continued pharmacological investigations aimed at identifying further, and more selective, agonists and antagonists of Panx1 will be key to furthering our understanding of Panx1 function.

Acknowledgements

We are indebted to Elizabeth Martin for molecular and cell biology support and Austen Sitko for cell culture and transfections.

References

Baranova A, Ivanov D, Petrash N, Pestova A, Skoblov M, Kelmanson I, Shagin , Naarenko S, Geraymovych E, Litvin O, Tiunova A, Born TL, Usman N, Staroverov D, Lukyanov S and Panchin Y (2004) The mammalian pannexin family is homologous to the invertebrate innexin gap junction proteins. *Genomics* **83:** 706-716.

Barbe MT, Monyer H and Bruzzone R. (2006) Cell-cell communication beyond connexins: the pannexin channels. *Physiology* **21:** 103-114.

Bruzzone R, Barbe MT, Jakob NJ and Monyer H (2005) Pharmacological properties of homomeric and heteromeric pannexin hemichannels expressed in Xenopus oocytes. *J Neurochem* **92:**1033-1043.

Bruzzone R, Hormuzdi SG, Barbe MT, Herb A and Monyer H (2003) Pannexins, a family of gap junction proteins expressed in brain. *Proc Natl Acad Sci USA* **100:**13644-13649.

Gelband CH, Greco PG and Martens JR (1996) Voltage-dependent chloride channels: invertebrates to man. *J Exp Zool* **275:**277-282.

Huang Y, Grinspan JB, Abrams CK and Scherer SS (2007a). Pannexin1 is expressed in neurons and glia but does not form functional gap junctions. *Glia* **55:**46-56.

Huang YJ, Maruyama Y, Dvoryanchikov G, Pereira E, Chaudhari N and Roper SD (2007b) The role of pannexin 1 hemichannels in ATP release and cell-cell communication in mouse taste buds. *Proc Natl Acad Sci USA* **104:** 6436-6441.

Iglesias R, Locovei S, Roque AP, Alberto AP, Dahl G, Spray DC and Scemes E (2008) P2X7 receptor-pannexin1 complex: Pharmacology and signalling. *Am J Physiol Cell Physiol* [doi:10.1152/ajpcell.00228.2008]

Jackson PS and Strange K (1995) Characterization of the voltage-dependent properties of a volume-sensitive anion conductance. *J Gen Physiol* **105:** 661-677.

Kidd JF and Thorn P (2000) Intracellular Ca^{2+} and Cl^- channel activation in secretory cells. *Annu Rev Physiol* 493-513.

Locovei S, Bao L and Dahl G (2006a) Pannexin 1 in erythrocytes: function without a gap. *Proc Natl Acad Sci USA* **103:**7655-7659.

Locovei S, Wang J and Dahl G (2006b) Activation of pannexin 1 channels by ATP through P2Y receptors and by cytoplasmic calcium. *FEBS Lett* **580:** 239-244.

Panchin Y (2005) Evolution of gap junction proteins – the pannexin alternative. *J exp Biol* **208:** 1415-1419.

Pelegrin P and Surprenant A (2006) Pannexin 1 mediates large pore formation and interleukin-1beta release by the ATP-gated $P2X_7$ receptor. *EMBO J* **25:**5071-5082.

Pelegrin P and Surprenant A (2007) Pannexin 1 couples to maitotoxin- and nigericin-induced interleukin-1beta release through a dye uptake-independent pathway. *J Biol Chem* **282:** 2386-2394.

Roger S, Pelegrin P and Surprenant A (2008) Facilitation of $P2X_7$ receptor currents and membrane blebbing via constitutive and dynamic calmodulin binding. *J Neurosci* **28:** 6393-6401.

Scemes E, Suadicani SO, Dahl G and Spray DC (2007) Connexin and pannexin mediated cell-cell communication. *Neuron Glia Biol* **3:** 199-208.

Silverman W, Locovei S and Dahl G (2008) Probenecid, a gout remedy, inhibits pannexin-1 channels. *Am J Physiol Cell Physiol* [doi:10.1152/ajpcell.00227.2008]

Strange K, Emma F and Jackson PS (1996) Cellular and molecular physiology of voltage-sensitive anion channels. *Am J Physiol* **270:**C711-730.

Vanden Abeele F, Bidaux G, Gordienko D, Beck B, Panchin YV, Baranova AV, Ivanov DV, Skryma R and Prevarskaya N (2006) Functional implications of calcium permeability of the channel formed by pannexin 1. *J Cell Biol* **174:**535-546.

Young MT, Pelegrin P and Surprenant A (2007) Amino acid residues in the P2X7 receptor that mediate differential sensitivity to ATP and BzATP. *Mol Pharmacol* **71:** 92-100.

Footnotes

This work was supported by the BBSRC and AstraZeneca Charnwood UK.

Legends for Figures

Figure 1. Characterization of human Panx-1 variants. **A**, multiple alignment of the different human Panx-1 variants (Panx1a AAK91713, Panx1b NP_056183, Panx1bv FM201789) with mouse Panx1 (NP_062355) corresponding to the residues 372 – 407 of the intracellular C-terminus in human Panx1a. **B**, expression profile of Panx-1 variants by RT-PCR in different human cell lines and in brain, note the lack of Panx-1a expression. **C**, detection of Panx1b and Panx1bv by PCR in the genomic DNA of HeLa and THP-1 cells. Expression vectors for the different Panx1 variants were used as a positive control to confirm the specific amplification by the different oligonucleotide combinations (**B,C**). **D**, cellular localization of the different Panx1-ee tagged variants expressed in HEK293 by confocal microscopy, note similar membrane localization for all variants.

Figure 2. Functional expression of mouse and human Panx1. A, Currents in response to voltage steps from -120 to 80 mV and voltage ramps from -120 to 80 mV recorded from HEK293 cells expressing mPanx1. Lanthanum (2 mM) blocks inward but not outward current while CBX (30 μM) blocks only outward current. We have defined the Panx1 current as the CBX-sensitive component. **B,** shows CBX inhibition of human Panx1 currents and **C** shows rapid onset of CBX inhibition. **D,** Frequency of expression of Panx1 currents from cells transfected with the indicated constructs; in all transfections equivalent percentage of cells (> 80%) expressed Panx1 protein as determined by immunohistochemistry (as per Supplemental Figure 1). **E,** Mean current at 70 mV recorded from cells expressing Panx1 currents; there were no significant differences among the human variants or between mouse and human Panx1 currents.

Figure 3. Panx1 currents are not modulated by calcium. **A,** mPanx1 currents recorded with low internal calcium (< 1 nM), high internal calcium (720 nM) with 2 mM external calcium, or low internal calcium and zero external calcium. **B,** Activation of Trp-like currents in response to U73122 (10 μM, blue traces recorded at 1 min intervals). **C,** Currents in absence (black trace) or presence of 2 mM lanthanum (blue traces at 1 min intervals) which show no change in CBX-sensitive Panx1 current over this time course. **D,** Currents in U73122 + lanthanum (blue traces at 1 min intervals); Panx1 currents are now inhibited. **E,** The PLC-inactive analogue, U73343 (10 μM), also inhibited Panx1 currents.

Figure 4. Kinetics of calcium-independent inhibition of Panx1 currents by U73122 and U73343. Summary of all experiments as illustrated in Figure 4. **A,** shows inhibition by U73122 as a function of time in different internal/external calcium concentrations; there were no significant differences. **B,** Kinetics of inhibition by U73122 and U73343; inhibition by U73343 was slower than U73122 but same maximum inhibition occurred with either compound.

Figure 5. Inhibition of Panx1 currents by some chloride channel/anion transporter inhibitors. **A,** shows two examples of concentration dependent inhibition of mPanx1 currents by NPPB (left) and SITS (right); note NPPB inhibited inward as well as outward current; lanthanum (2 mM) present throughout. **B,** Concentration-inhibition curves for inhibitory compounds; each point is mean ± s.e.m. of 5 – 12 points. **C,** Histogram shows

mean currents in the presence of 100 μM of each of the compounds except for CBX which was 50 μM.

Figure 6. Extracellular nucleoside triphosphates inhibit Panx1 currents. Voltage steps (**A**) and ramps (**B**) in control and presence of ATP as indicated. **C,** Concentration inhibition curves for ATP, UTP and GTP inhibition of mPanx1 as indicated; $n = 5 – 14$ for each point. **D,** Currents recorded with high intracellular ATP (20 mM); no differences in peak current or inhibition by extracellular ATP or CBX were observed. **E,** Panx1 currents in presence of maximum concentrations of nucleotides, nucleosides and phosphates as indicated.

Figure 7. Actions of Panx1 inhibitors on ATP-evoked currents in cells co-expressing Panx1 and $P2X_7$ receptor. A, Examples of ATP-evoked currents in presence and absence of CBX, NPPB and MFQ as indicated; currents were slightly increased or unaltered. **B,** Example of ATP-evoked currents in absence and presence of DIDS. **C,** Summary of all experiments as illustrated in **A,B**; results for NPPB and MFQ at each of the three $P2X_7$Rs are pooled because there was minimal or no effect while inhibition by DIDS is shown for each species, $n = 5 – 18$ for each point. DIDS IC_{50} values were 90 ± 4 μM, 130 ± 12 μM and 195 ± 21 μM for rat, mouse and human $P2X_7$R respectively.

JPET Fast Forward. Published on November 20, 2008 as DOI: 10.1124/jpet.108.146365
This article has not been copyedited and formatted. The final version may differ from this version.

	IC_{50} values (μM)		
	mouse panx1	human panx1	effect on $P2X_7R$ current
CBX	4 ± 0.6 (29)	2 ± 1 (18)	5-10% increase (14)
DIDS	9 ± 2 (6)	11 ± 2 (4)	receptor antagonist*
NPPB	15 ± 2 (12)	21 ± 4 (4)	15% increase (6)
SITS	11 ± 3 (6)	13 ± 3 (4)	not examined
IAA-94	95 ± 6 (5)	not examined	not examined
FFA	> 1000 (6)	> 1000 (8)	No effect (5)
NFA	> 1000 (5)	> 1000 (4)	No effect (5)
Probenecid	352 ± 31 (5)	360 ± 21(3)	No effect (3)
MFQ	no effect**(12)	no effect**(5)	no effect** (12)
ATP	752 ± 42 (8)	825 ± 56 (12)	receptor agonist***
UTP	1256 ± 56 (7)	1350 ± 60 (4)	No effect (4)
GTP	1290 ± 87 (6)	1420 ± 108 (3)	No effect (4)

Table 1. IC_{50} values (μM) for inhibition of panx1 currents and comparison to actions of these compounds at $P2X_7R$. Numbers in parentheses are n values. * IC_{50} for DIDS at rat, mouse and human $P2X_7R$ = 90, 130 and 195 μM respectively (see Fig. 8). ** Concentrations from 1 nM to 10 μM.). ***EC_{50} for activation at rat, mouse and human $P2X_7R$ = 640 ± 22 μM, 985 ± 35 μM, and 952 ± 120 μM respectively. Numbers of cells tested are indicated in parentheses.

A

```
hPanx1a   MIKMDVVDGKTPMSAEMR-EEQGNQTAELQ----DSETKAN 407
hPanx1b   MIKMDVVDGKTPMSAEMR-EEQGNQTAELQGMNIDSETKAN 411
hPanx1bv  MIKMDV-DGKTPMSAEMR-EEQGNQTAELQGMNIDSETKAN 410
mPanx1    MIKMDIIDGKIPTSLQTKGEDQGSQRVEFKDLDLSSEARAN 411
          *****..*** * * . . *.** *  * .     **..**
```

B

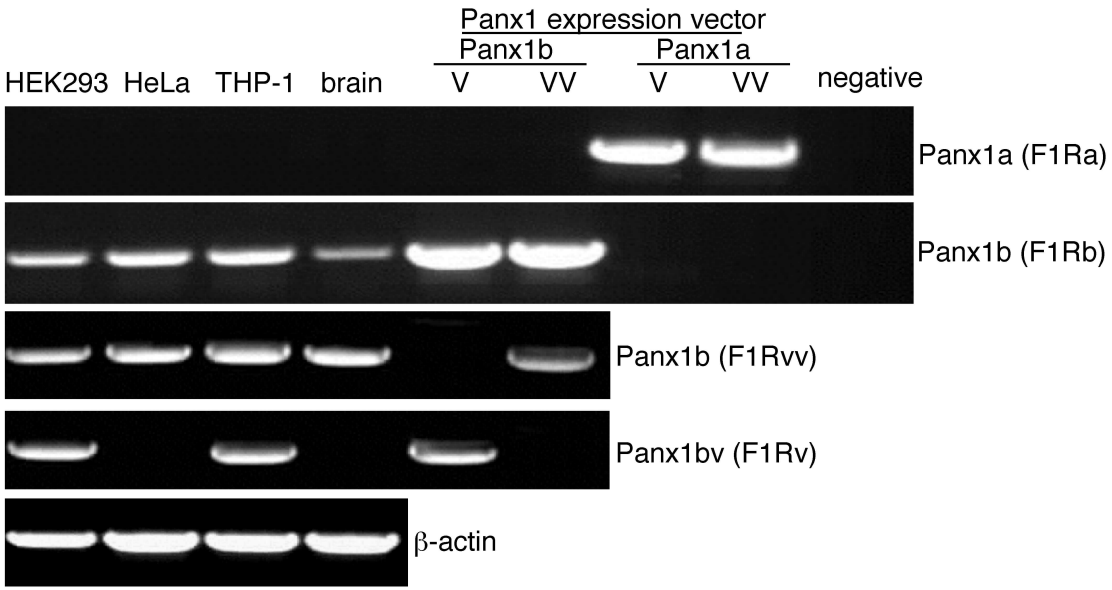

C

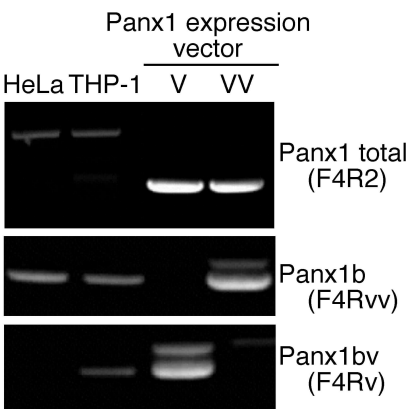

D

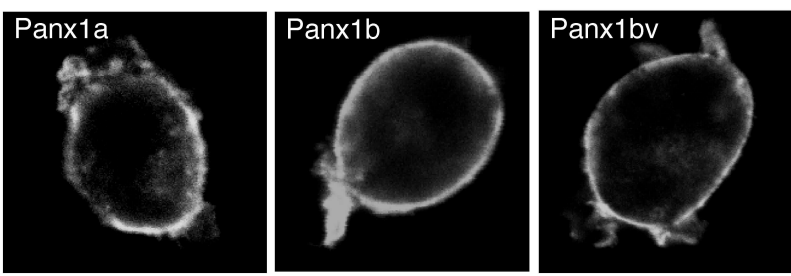

Figure 2

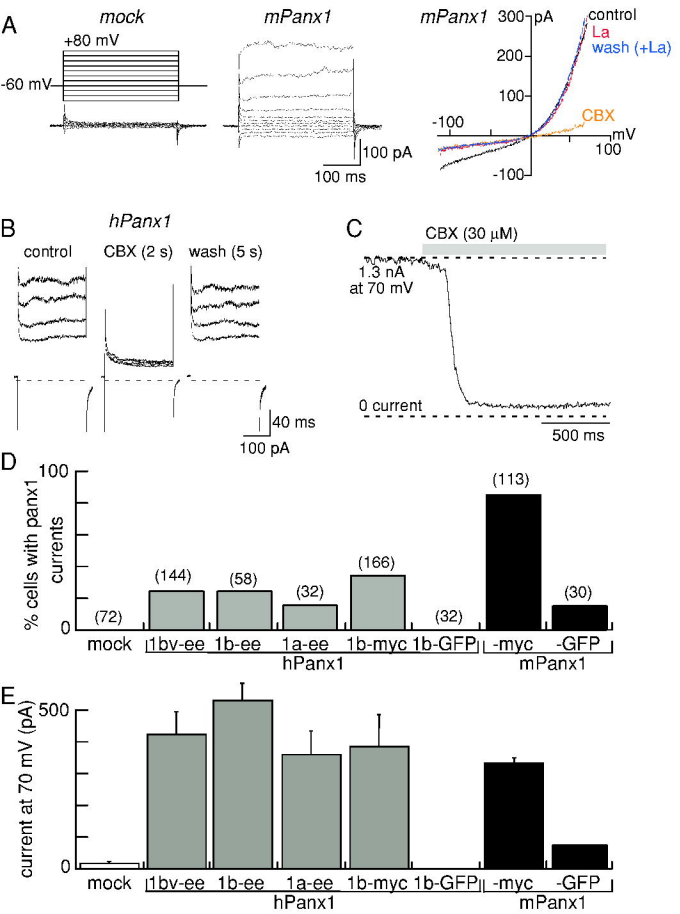
A
mock
+80 mV
-60 mV
mPanx1
100 pA
100 ms
mPanx1
300 pA
control
La
wash (+La)
200
100
-100
CBX
mV
100
-100
B
hPanx1
control
CBX (2 s)
wash (5 s)
40 ms
100 pA
C
CBX (30 μM)
1.3 nA
at 70 mV
0 current
500 ms
D
% cells with panx1 currents
100
0
(72)
(144)
(58)
(32)
(166)
(32)
(113)
(30)
mock
1bv-ee
1b-ee
1a-ee
1b-myc
1b-GFP
-myc
-GFP
hPanx1
mPanx1
E
current at 70 mV (pA)
500
0
mock
1bv-ee
1b-ee
1a-ee
1b-myc
1b-GFP
-myc
-GFP
hPanx1
mPanx1

Figure 3

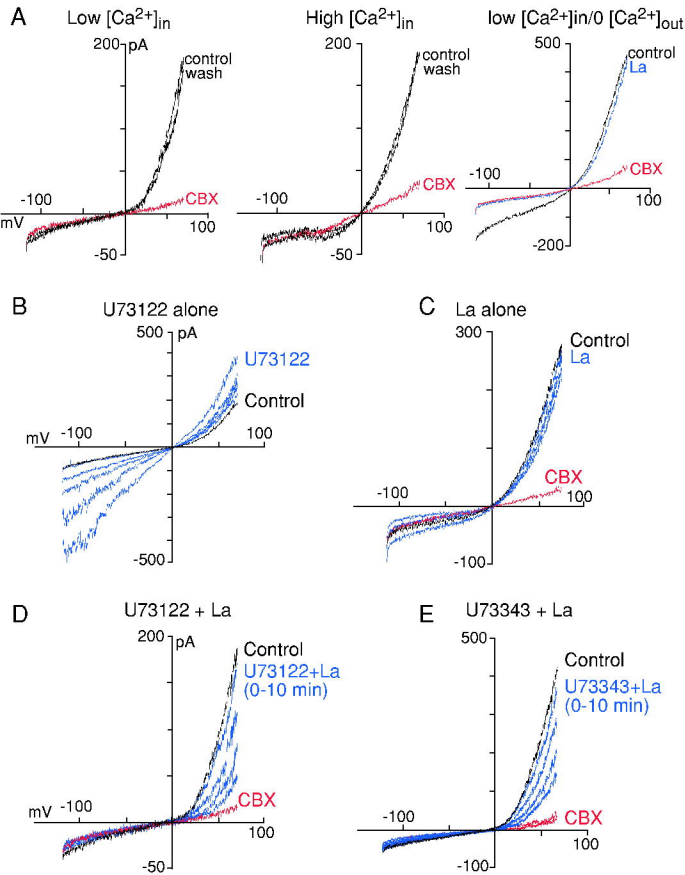
A
Low [Ca2+]in
200 pA
control
wash
CBX
-100
mV
100
-50
High [Ca2+]in
200
control
wash
CBX
-100
100
-50
low [Ca2+]in/0 [Ca2+]out
500
control
La
CBX
-100
100
-200
B
U73122 alone
500 pA
U73122
Control
mV -100
100
-500
C
La alone
300
Control
La
CBX
-100
100
-100
D
U73122 + La
200 pA
Control
U73122+La
(0-10 min)
CBX
mV -100
100
-50
E
U73343 + La
500
Control
U73343+La
(0-10 min)
-100
CBX
100
-100

Figure 4

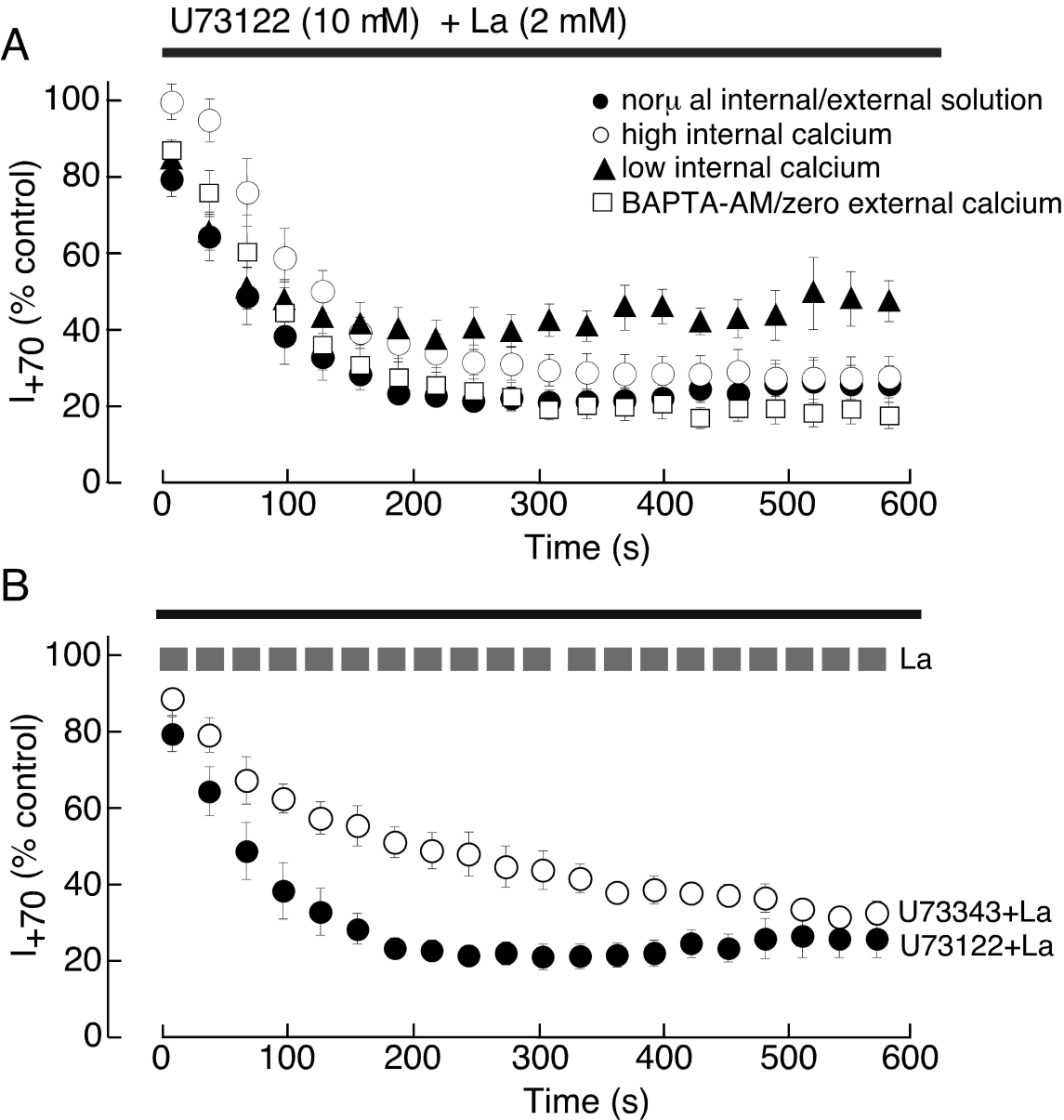
A
U73122 (10 mM) + La (2 mM)
normal internal/external solution
high internal calcium
low internal calcium
BAPTA-AM/zero external calcium
I+70 (% control)
Time (s)
B
La
U73343+La
U73122+La
I+70 (% control)
Time (s)

Figure 5

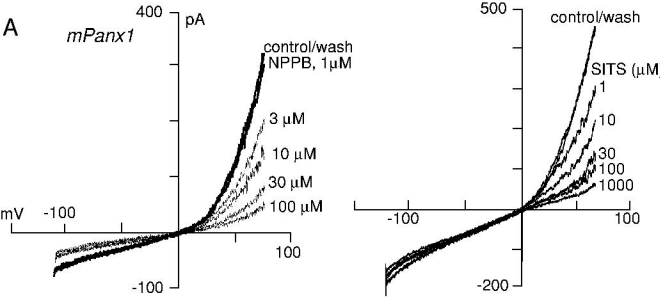
A
mPanx1
400
pA
control/wash
NPPB, 1μM
3 μM
10 μM
30 μM
100 μM
mV
-100
100
-100
500
control/wash
SITS (μM)
1
10
30
100
1000
-100
100
-200

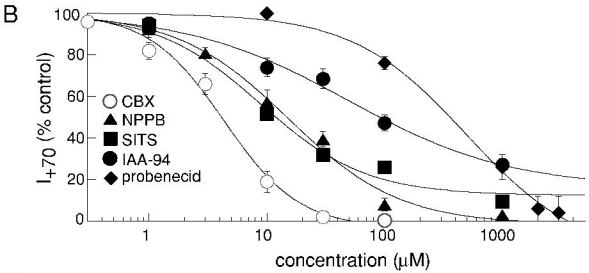
B
100
80
60
40
20
0
I+70 (% control)
CBX
NPPB
SITS
IAA-94
probenecid
1
10
100
1000
concentration (μM)

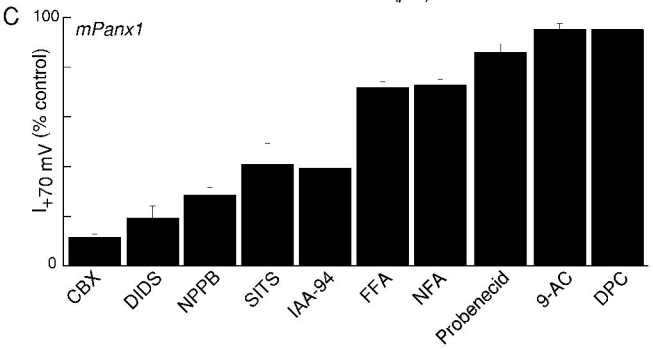
C
mPanx1
100
0
I+70 mV (% control)
CBX
DIDS
NPPB
SITS
IAA-94
FFA
NFA
Probenecid
9-AC
DPC

Figure 6

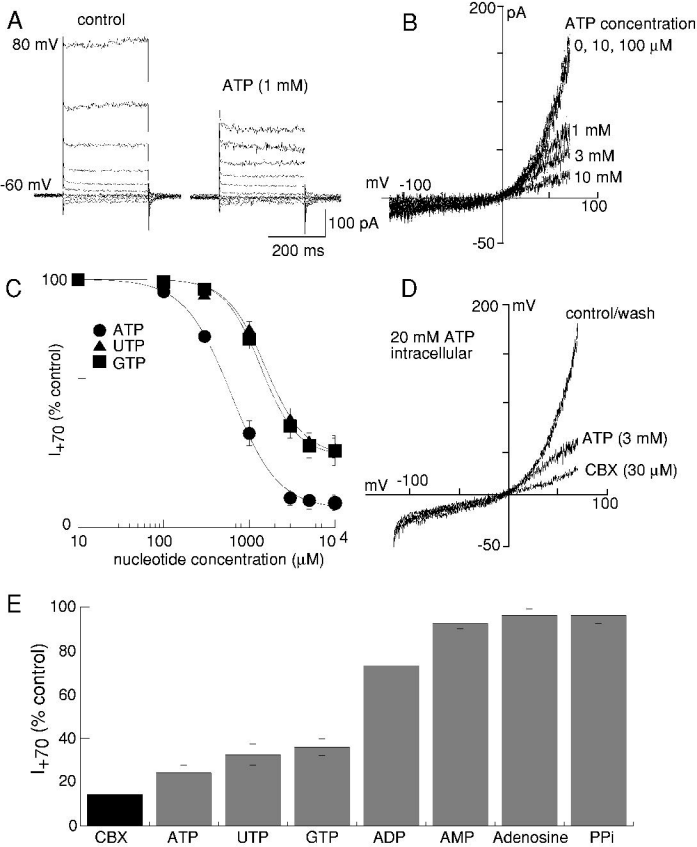
A
control
80 mV
-60 mV
ATP (1 mM)
100 pA
200 ms
B
200 pA
ATP concentration
0, 10, 100 μM
1 mM
3 mM
10 mM
mV -100
100
-50
C
100
ATP
UTP
GTP
I+70 (% control)
0
10
100
1000
10 4
nucleotide concentration (μM)
D
200 mV
control/wash
20 mM ATP
intracellular
ATP (3 mM)
CBX (30 μM)
mV -100
100
-50
E
I+70 (% control)
100
80
60
40
20
0
CBX
ATP
UTP
GTP
ADP
AMP
Adenosine
PPi

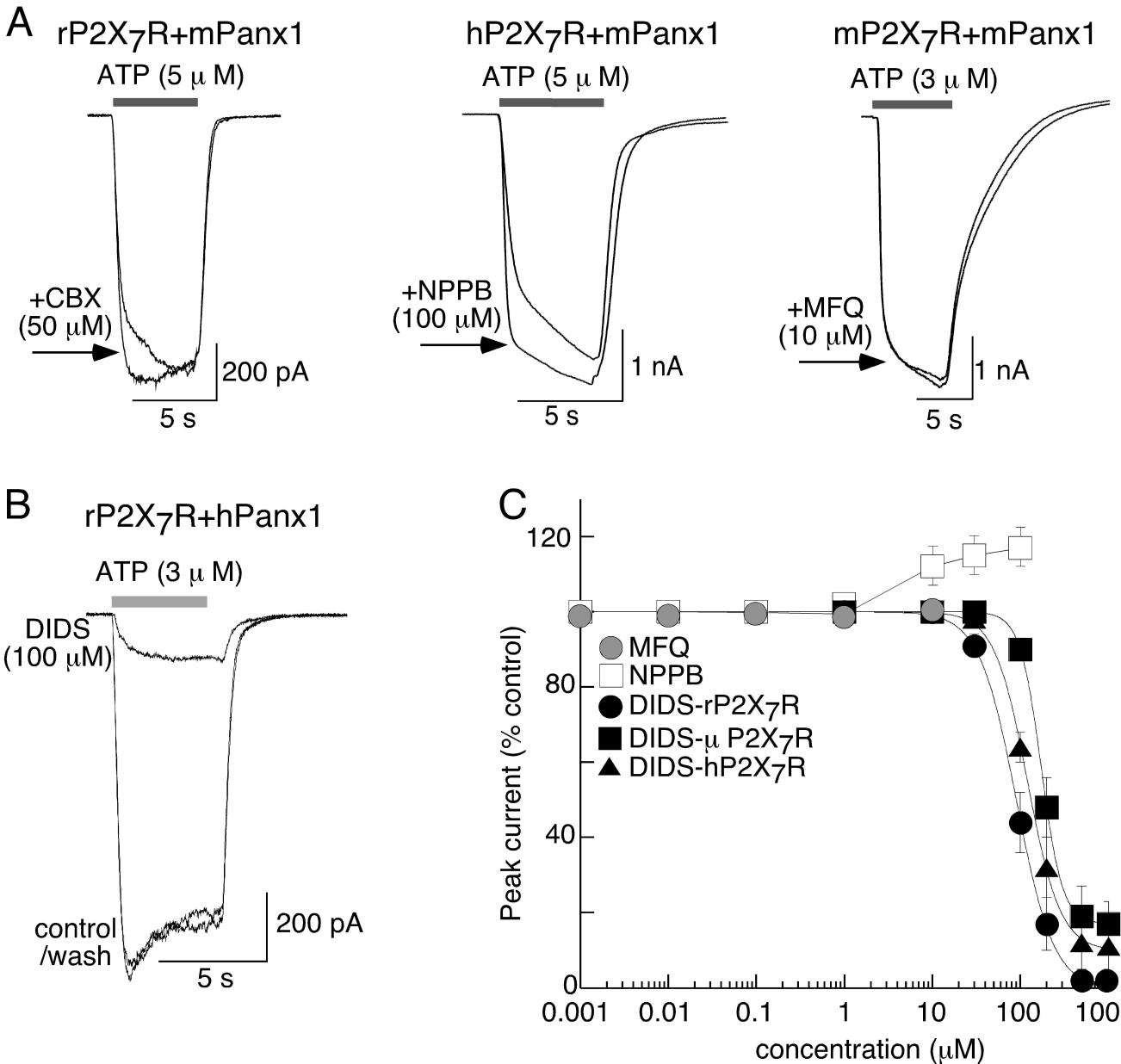
A
rP2X7R+mPanx1
ATP (5 μ M)
+CBX
(50 μM)
200 pA
5 s
hP2X7R+mPanx1
ATP (5 μ M)
+NPPB
(100 μM)
1 nA
5 s
mP2X7R+mPanx1
ATP (3 μ M)
+MFQ
(10 μM)
1 nA
5 s
B
rP2X7R+hPanx1
ATP (3 μ M)
DIDS
(100 μM)
control
/wash
200 pA
5 s
C
Peak current (% control)
120
80
40
0
MFQ
NPPB
DIDS-rP2X7R
DIDS-μ P2X7R
DIDS-hP2X7R
0.001
0.01
0.1
1
10
100
1000
concentration (μM)